Chemical Physics 72 (1982) 371–379
North-Holland Publishing Company

LASER-INDUCED ULTRASONICS: A DYNAMIC HOLOGRAPHIC APPROACH TO THE MEASUREMENT OF WEAK ABSORPTIONS, OPTOELASTIC CONSTANTS AND ACOUSTIC ATTENUATION

R.J. Dwayne MILLER, Roger CASALEGNO *, Keith A. NELSON ** and M.D. FAYER
Department of Chemistry, Stanford University, Stanford, California 94305, USA

Received 10 May 1982

A quantitative comparison of experiment to the theoretical descriptions of two mechanisms for the optical generation of tunable ultrasonic waves is presented. Crossed picosecond excitation pulses drive the acoustic response either by stimulated Brillouin scattering or absorptive heating. Bragg diffraction from the induced acoustic grating permits detection of the ultrasonic disturbance and measurement of weak absorptions, optoelastic constants and acoustic attenuation. The methods are applied to various liquids. Measurement of the C–H stretch fifth overtone absorption spectrum of pure benzene in a short path length cell is demonstrated.

1. Introduction

Recently, a technique for the optical excitation and optical detection of tunable ultrasonic waves in transparent or absorbing media was reported [1–4]. The technique, called laser-induced phonons or LIPS, involves crossed picosecond laser pulses which set up an optical interference pattern inside the sample and excite counterpropagating ultrasonic waves whose wavelength and orientation match those of the interference pattern (see fig. 1). The ultrasonic waves are detected by Bragg diffraction of a third laser pulse [4].

Two distinct mechanisms for ultrasonic wave generation have been demonstrated. In optically absorbing samples, radiationless relaxation heats the optical interference maxima and thermal expansion drives the acoustic response [1]. The strength of the response is proportional to the absorption coefficient. In transparent samples, stimulated Brillouin scattering (electrostriction) provides the necessary coupling between the electromagnetic field of the crossed excitation pulses and the acoustic field of the medium [2,3,5]. The am-

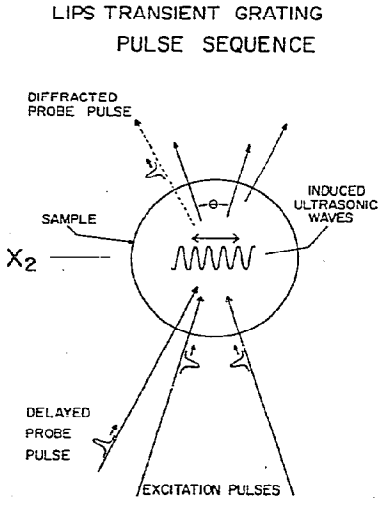

Fig. 1. Schematic illustration of the LIPS transient grating experiment. The crossed excitation pulses generate counterpropagating acoustic waves (phonons) with the wavelength and orientation of the optical interference pattern. Phonon-induced changes in the index of refraction create a diffraction grating which Bragg diffracts the delayed probe pulse. The phonon wavelength is given by $\Lambda = \lambda/2 \sin(\theta/2)$, where λ is the excitation wavelength and θ is the angle between the beams. The phonon frequency is continuously tunable by varying θ.

* Permanent address: Laboratoire de Spectrometrie Physique, Université I, 38041, Grenoble, France.
** Permanent address: Chemistry Department, MIT, Cambridge, MA 02139, USA.

0301-0104/82/0000–0000/$ 02.75

plitude of the acoustic response is proportional to the electrostrictive (optoelastic) constant of the medium. If absorption is strong, the first mechanism dominates and electrostriction effects are negligible. If absorption is very weak – as in overtone absorption, for example – the effects of both mechanisms can be comparable in magnitude. Each mechanism is characterized by the distinct time dependence of its acoustic response [3]. Thus time-dependent Bragg diffraction of the variably delayed picosecond probe pulse allows experimental determination of which mechanism dominates in a particular system. This method of detection also permits the observation of acoustic attenuation, since the diffracted signal diminishes as the waves are damped.

In this paper, we present quantitative verification of the theoretical description of the LIPS effect. Measurements of an overtone absorption spectrum, optoelastic constants, and acoustic attenuation constants, obtained from LIPS data, are reported. In addition to quantitatively confirming the theoretical description, the experiments described below also demonstrate the usefulness of LIPS as a quantitative and convenient analytical tool. Some of the important features of the effect are the following: (1) The propagation direction of the acoustic waves is determined by the geometry of the laser excitation beams. Thus in anisotropic media, it is straightforward to make measurements in a variety of directions [1] without mechanical contact with the sample. Also, because it is unnecessary to make mechanical contact, measurements can be made on very small samples or on selected areas of a large sample. (2) The acoustic frequency is tunable over four orders of magnitude. With the current experimental apparatus, acoustic wavelengths from 0.1 to 1000 μm can be generated. (3) Using a laser pulse sequence, the acoustic waves can be amplified, cancelled or phase shifted [3]. This switching of the acoustic waves occurs virtually instantaneously relative to the time scale of an acoustic cycle. (4) As mentioned above, the acoustic amplitude can be related directly to absorption coefficients, optoelastic constants, and acoustic attenuation constants, offering alternate approaches for the determination of these parameters.

2. Theory

2.1. Acoustic wave generation

The theoretical description of the LIPS effect in anisotropic media, has been presented earlier [1–4]. In the heating mechanism [1], optical absorption into high-lying vibronic or vibrational levels followed by rapid radiationless relaxation images the crossed excitation pulses' interference pattern in the form of a periodic temperature distribution. The impulsive thermal expansion which results at the grating interference peaks launches counterpropagating acoustic waves along the grating direction. This results in an acoustic wavelength which is the same as that of the interference fringe spacing, given by

$$\Lambda = \lambda/2 \sin \tfrac{1}{2}\theta \,, \tag{1}$$

where λ is the wavelength in air of the excitation pulses, θ is defined as in fig. 1, and Λ is the acoustic wavelength, i.e. the grating fringe spacing.

The thermally induced acoustic strain, S_2, is given by [1]

$$S_2 = A \cos(k_2 x_2)[1 - \cos(\omega t)] \,, \tag{2}$$

where $k_2 = 2\pi/\Lambda$ is the acoustic wave vector, x_2 is the direction of propagation (see fig. 1) and ω is the acoustic frequency ($\omega/k_2 = v_p$, the speed of sound). The acoustic amplitude, A, is given by

$$A = (c_{11} + 2c_{12})\, a\, \Delta T_m k_2^2/6\omega^2\rho_0 \,, \tag{3}$$

where c_{11} and c_{12} are the material's elastic constants [6,7], a is the volume thermal expansivity [7], and ρ_0 is the normal density. ΔT_m is the temperature jump at the interference maxima

$$\Delta T_m = q\beta I_m/\rho_0 C_v \,, \tag{4}$$

where q (erg photon^{-1}) is the fraction of the absorbed photon's energy immediately deposited into the lattice by radiationless relaxation, β (cm^{-1}) is the absorptivity per unit length, I_m (photons cm^{-2}) is the integrated light intensity at the interference peaks and C_v (erg K^{-1} g^{-1}) is the constant-volume heat capacity.

The acoustic strain amplitude, A, as given in eq. (3) is for an isotropic solid continuum. In the liquid phase, this expression can be simplified since $c_{11} = c_{12}$, i.e. there is no shear component to the elasticity. With this,

$$A = K_s a \Delta T_m k_2^2/2\omega^2\rho_0 \,, \tag{5}$$

where K_S is the liquid's isentropic bulk modulus [7].

Inspection of eq. (2) shows that the qualitative features of the theoretical description of the LIPS effect include a time-dependent term due to the counterpropagation of the acoustic waves and a time-independent term which results from the non-propagating periodic temperature distribution. Since thermal diffusion occurs on a microsecond timescale, this temperature pattern can be considered time independent on the nanosecond time scale of the LIPS experiment.

Unlike the heating mechanism, the electrostriction mechanism [2–4] is a consequence of the direct coupling of the laser pulses' E field to the material's acoustic field. Previously, it has been demonstrated that the intersection of two different wavelength pulses in a sample at the correct angle, dictated by k conservation, produces an efficient conversion of light to sound energy [8]. The acoustic response is a single traveling wave with a frequency given by the difference frequency between the two laser pulses.

In the LIPS experiment, the two very short laser pulses, which intersect in the sample, are the same frequency. However, the inherent spectral width of the short pulses provides the required frequency difference and ensures that the phase matching condition is met at all angles of intersection, making this method a tunable source of ultrasound. Due to the symmetry of the excitation, the acoustic response will have wavevectors $\pm k_2$, i.e. a standing wave will be generated.

In the electrostriction case, the strain has the general form [2]

$$S_2 = -B\cos(k_2 x_2)\sin(\omega t)\,. \tag{6}$$

B, the acoustic amplitude arising from electrostriction, is given by

$$B = \frac{n^3 k_2 p_{12} I_m \exp(-2k_2^2 v_p^2/\Gamma^2)}{4 v_p \rho_0 c \gamma}, \tag{7}$$

where n is the index of refraction, c is the speed of light, Γ is the laser pulse spectral width, γ is the conversion factor, photon erg^{-1}, and p_{12} is the Pockels' optoelastic constant [9]. For short laser pulses, $\Gamma \gg k_2 v_p$ and the exponential term can be neglected.

In liquids, the optoelastic parameter usually measured is $\rho\,\partial n/\partial\rho$ [10–14], which can be related to Pockels' constants by the relation [15]

$$\rho\,\partial n/\partial\rho = \tfrac{1}{6} n^3 (p_{11} + 2p_{12})\,. \tag{8}$$

It can be shown [16] using standard acoustic theory [6] and experimental data [17] that for liquids,

$$p_{11} = p_{12}\,. \tag{9}$$

This condition states that it is impossible to induce birefringence in a liquid by an applied strain. There are exceptions to this for certain liquids [18]. However, for most liquids, including those studied below, eq. (9) is valid. In this case,

$$\rho\,\partial n/\partial\rho = \tfrac{1}{2} n^3 p_{12} \tag{10}$$

and the electrostrictive acoustic amplitude becomes

$$B = k_2 \rho(\partial n/\partial\rho) I_m / 2 v_p \rho_0 \gamma c\,. \tag{11}$$

As described in detail below, eqs. (5) and (11) allow quantitative verification of the theoretical treatments of the LIPS generating mechanisms by comparing known values of the optoelastic constants of liquids with those obtained from LIPS measurements.

In a number of experiments, both the absorption and electrostriction mechanisms contribute to the acoustic strain. In these situations, the total strain is just the sum of eqs. (2) and (6), i.e.

$$S_2 = \cos(k_2 x_2)\{A[1 - \cos(\omega t)] - B\sin(\omega t)\}\,, \tag{12}$$

where the relative contributions of the two mechanisms are determined by the magnitudes of A and B.

2.2. Experimental observables

The observable in a LIPS experiment is the intensity of the diffracted probe pulse due to the induced acoustic disturbance. The efficiency of light diffraction from a phase grating in the Bragg limit [19–21] is given by

$$\eta = \sin^2(\pi n_1 d/\lambda\cos\phi_0)\,, \tag{13}$$

where η is the diffraction efficiency, n_1 is the peak–null difference in the refractive index arising from the acoustic disturbance, d is the grating thickness, and ϕ_0 is the Bragg diffraction angle. This relation is for s-polarized light. In the experiments discussed below, diffraction is from pure ultrasonic phase gratings and eq. (13) applies. Diffraction from mixed amplitude and phase gratings in LIPS experiments has been described previously [4].

The density dependence of the refractive index is given by

$$\delta n = (\partial n/\partial \rho)\,\delta\rho\,, \tag{14}$$

where δn is the change in n, and the change in density, $\delta\rho$, is related to the acoustic strain by [6]

$$\delta\rho = -\rho S_2\,. \tag{15}$$

The peak–null difference n_1 is therefore

$$n_1 = -\rho(\partial n/\partial\rho)(S_{2\,\text{peak}} - S_{2\,\text{null}})\,, \tag{16}$$

and inserting this into eq. (13) gives, for $\eta \ll 1$,

$$\eta = \left[\pi\rho\,\frac{\partial n}{\partial\rho}\,\frac{S_{2\,\text{peak}} - S_{2\,\text{null}}}{\lambda\cos\phi_0}\,d\right]^2. \tag{17}$$

The mechanisms of phonon generation manifest themselves in the term S_2, the oscillatory nature of which gives rise to the characteristic LIPS modulation of the diffracted signal. The theoretical description of S_2 given in section 2.1 provides the direct connection between the modulation of the diffracted signal and the samples' absorption cross section and optoelastic constant.

2.2.1. Measurement of weak absorption

If the sample's optical absorption is very weak, the contributions of both mechanisms to the total strain are comparable. The heating mechanism results in material displacement away from the interference peaks (expansion), while for most liquids, it has been determined that the acoustic fields driven electrostrictively have a net material displacement towards the interference peaks (contraction). Thus the contributions to the acoustic disturbance for the heating and electrostriction mechanisms are usually opposite in sign as written in eq. (12). Taking this into account in the peak–null difference in strain yields

$$\eta = \{(2\pi d/\lambda\cos\phi_0)\,\rho(\partial n/\partial\rho) \times \{A[1-\cos(\omega t)] - B\sin(\omega t)\}\}^2\,. \tag{18}$$

$\eta(t) \propto (A-B)^2$ at $t = \frac{1}{4}\tau, \frac{5}{4}\tau, \ldots, (j+\frac{1}{4})\tau$, where j is an integer and τ is the acoustic period $(2\pi/\omega)$. At $t = \frac{3}{4}\tau$, $\frac{7}{4}\tau \ldots, (j+\frac{3}{4})\tau$, $\eta(t) \propto (A+B)^2$. Measuring the diffraction efficiency at two appropriate times gives the magnitude of A relative to B, e.g.

$$\frac{A}{B} = \frac{\eta^{1/2}(\frac{3}{4}\tau) - \eta^{1/2}(\frac{1}{4}\tau)}{\eta^{1/2}(\frac{3}{4}\tau) + \eta^{1/2}(\frac{1}{4}\tau)}, \qquad A < B\,. \tag{19}$$

Measuring the ratio A/B is useful for two reasons. First, B is basically independent of wavelength even for substantial changes in wavelength. Therefore a plot of A/B versus λ yields the absorption spectrum. In addition, both A and B are linear in the excitation pulse intensity. Thus the ratio A/B is independent of the laser intensity and is directly proportional to the absorption strength. If B is known, or if a suitable absorption standard is used (as described below), the molar extinction coefficient as a function of wavelength can be obtained from a LIPS experiment for very weakly absorbing samples. This is in effect a type of coherent optoacoustic spectroscopy in which the thermal energy is channeled into a single acoustic frequency and detected by Bragg diffraction.

2.2.2. Measurement of optoelastic constants

As can be seen from eqs. (18) and (11), the signal depends on $\rho\,\partial n/\partial\rho$. This constant can be determined from LIPS experiments either by utilizing an absorptive standard or an electrostrictive reference. In the former case, a dilute absorption standard is used to produce a known acoustic strain amplitude, A, through absorptive heating. Measuring A/B as in eq. (19) then gives B, and $\rho\,\partial n/\partial\rho$ can be calculated from eq. (11). Explicitly, using eqs. (11), (5), and (4) and the relation $K_s = v_p^2\rho_0$, we have

$$\rho\,\partial n/\partial\rho = (B/A)\,v_p a\beta c q\gamma/k_2 C_v\,. \tag{20}$$

In eq. (20), a, β, c, C_v, q and γ are known constants and the remaining parameters are obtained directly from the LIPS experiment. Measurement of optoelastic constants in this manner provides a means to rigorously test both the absorption and electrostriction models of LIPS generation. An experiment of this type is described below.

In the limit of zero absorption ($A = 0$), optoelastic constants can be obtained by a second method which is simpler. Samples with unknown constants have their diffraction efficiency compared to a reference sample with a known constant. Rearrangement of eqs. (18) and (11) with $A = 0$ gives

$$\left[\rho\,\frac{\partial n}{\partial\rho}\right]_u = \left[\left(\frac{\eta_u(\frac{1}{4}\tau_u)}{\eta_r(\frac{1}{4}\tau_r)}\right)^{1/2}\frac{(v_p\rho_0)_u}{(v_p\rho_0)_r}\right]^{1/2}\left[\rho\,\frac{\partial n}{\partial\rho}\right]_r, \tag{21}$$

where the subscripts u and r stand for unknown and reference, respectively. This procedure is demonstrated below.

2.2.3. Measurement of acoustic attenuation

Typically, the intensity of the oscillating LIPS signal gradually dies away due to acoustic attenuation. Measurement of the rate of decay allows determination of the attenuation rate constant. It is most convenient to compare the intensities of the diffraction maxima in successive acoustic cycles, and to calculate the attenuation rate constant, α, as

$$\alpha = -\frac{\ln(h_j^{1/2}/h_i^{1/2})}{v_p\tau(j-i)}, \qquad (22)$$

where $j > i$ and h_j and h_i are the experimentally measured LIPS diffraction maxima in the jth and ith acoustic cycles. Since attenuation normally varies as the square of the acoustic frequency ν [22], the quantity α/ν^2 is reported.

At ultrasonic frequencies, acoustic attenuation in many liquids occurs on a nanosecond time scale, making LIPS a convenient technique for attenuation measurements. In applying LIPS to the measurement of other experimental observables, corrections for acoustic attenuation may be necessary. We note that attenuation effects during the excitation pulses (<100 ps) are almost always negligible and have not been accounted for in the theoretical treatment of the LIPS excitation mechanisms; these could be included if desired [2].

3. Experimental

The details of the laser system are schematically illustrated in fig. 2. The laser is an acoustooptic Q-switched and mode-locked Nd:YAG system which produces 1.06 μm pulse trains at 400 Hz. Single pulses of 100 ps duration and ≈45 μJ in energy are selected by a Pockels cell. The selected single pulse is then frequency doubled to produce 532 nm, 70 ps, 20 μJ, TEM_{00} pulses. The remaining IR pulse train is also doubled to produce a green pulse train which synchronously pumps a dye laser. The dye laser is capable of providing ≈15 μJ, 30 ps single pulses in the wavelength range of 550–700 nm. Frequency narrowing of these pulses to ≈1 cm^{-1} is accomplished by two intracavity etalons. A dye laser single pulse is selected by cavity dumping with a Pockels cell.

Depending on the experiment, either the dye or the green (532 nm) single pulse is passed through a

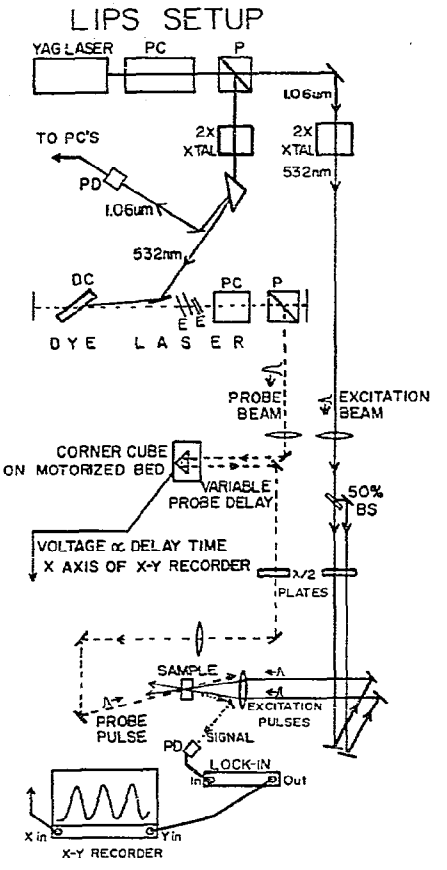

Fig. 2. Transient grating experimental arrangement. A single 1.06 μm pulse is selected from the Nd:YAG mode-locked pulse train and frequency doubled to 532 nm. The rest of the pulse train is frequency doubled to synchronously pump a tunable dye laser. The Bragg-diffracted part of the probe pulse is the transient grating signal. Either the 532 nm pulse or the dye laser pulse is split into the two excitation pulses and recombined at the sample to generate the acoustic response (532 nm excitation shown in diagram). The other pulse probes the induced ultrasonic grating after variable delay. PC ≡ Pockels cell; P ≡ polarizer; PD ≡ photodiode; DC ≡ dye cell; E ≡ etalon; BS ≡ beamsplitter.

50% beamsplitter, and the resulting two pulses are recombined to form the interference pattern which excites the acoustic waves. The other single pulse becomes the probe which is brought in at the appropriate angle for Bragg diffraction. Time resolution is obtained by variably delaying the probe pulse. A

retroreflector is drawn along a precision optical rail by a motor which provides continuous scanning of the probe delay. A ten-turn potentiometer, also driven by the motor, provides a voltage proportional to the probe delay. This voltage drives the x axis of an $x-y$ recorder. The diffracted signal is detected by a large-area photodiode and a lock-in amplifier. The output of the lock-in drives the y axis of the recorder. When the delay-line motor is run, a time-resolved plot of the diffracted signal is obtained.

In the LIPS measurements of the fifth vibrational overtone of benzene (described below), the diffracted intensities at fixed probe delays were recorded as a function of the excitation wavelength. In this experiment, the tunable dye laser provided the excitation pulses. The spectrum was recorded between 590 and 620 nm, point by point.

The elastooptic constant of ethanol at 532 nm was measured using malachite green oxalate (MG) (Eastman Kodak) as an absorption standard. The MG absorptivity was measured at moderate concentrations with a Cary 17 spectrometer and the low absorptivity standard was obtained by dilution. Elastooptic constants of other liquids were determined using ethanol as the electrostrictive reference. In this case, two matched 1 cm cuvettes were used, one for the reference and one for the unknown. This allowed rapid measurement of diffraction intensities of both sample and reference by moving a translation stage which brought one, then the other cuvette into the beam paths. Laser power drift was less than 1% between measurements.

To obtain accurate measurements of acoustic attenuation constants, it was found necessary to take into consideration the gaussian spatial profile of the excitation pulses. This was accomplished by making the probe spot size one-half the size of the excitation spot size and making the excitation angle large enough to provide a significant number of fringes (>15) within the probe spot size.

The focusing parameters, used in all the experiments, were an $\approx$200 μm spot size at the beam waist for the excitation pulses and an $\approx$100 μm spot size for the probe. The probe was focused by a lens its own focal length away to ensure a constant spot size as the delay line was scanned. The power dependence of the signal was checked routinely and was always found to be linear in the probe intensity and quadratic in the excitation intensity as expected (see eq. (17), i.e. $\Delta S \propto I_{ex}$). Only the first order of diffraction was monitored and diffraction efficiencies were on the order of 10^{-5}–10^{-6}.

4. Results and discussion

The existence of two different mechanisms for the generation of the LIPS effect is illustrated by the influence of MG concentration in ethanol on the time dependence of the signal, as shown in fig. 3. The 532 nm excitation pulses are strongly absorbed by MG and are basically not absorbed by ethanol. Malachite green, having a 2 ps lifetime [23] and a zero fluorescence quantum yield in EtOH deposits heat into the solution and drives the acoustic response thermally. All the excited MG molecules return to the ground state within the pulse duration such that the probe is diffracted solely by the ultrasonic phase grating. This permits direct comparison of the signal in EtOH with and without MG.

In fig. 3, the important feature is the frequency of oscillation in the signal. The grating fringe spacing (2.47 μm) and the sound velocity of EtOH [10] (1.14×10^5 cm s^{-1}), give an acoustic period of 2.13 ns. In pure ethanol (fig. 3a), the signal vanishes every 1.07 ns (exactly twice each acoustic cycle), and the maxima occur at $t = \frac{1}{4}\tau, \frac{3}{4}\tau$, etc. This demonstrates that the acoustic disturbance has the same form as given in eq. (6) for the electrostriction mechanism. Fig. 3c shows data from a 5×10^{-5} M solution of MG with all other conditions identical to those for fig. 3a. Now the signal vanishes once every acoustic cycle, with the peaks located at $t = \frac{1}{2}\tau, \frac{3}{2}\tau$, etc. These data demonstrate that the acoustic disturbance is given by eq. (2) and results from the absorption mechanism. With high MG concentrations, the magnitude of the acoustic disturbance generated thermally by absorption overwhelms the electrostrictive effect and only the absorptive heating mechanism is observed. In the absence of absorption, as in pure ethanol, only the electrostrictive mechanism is observed. In intermediate cases, as shown in fig. 3b, where the effects of absorption and electrostriction are of comparable magnitudes, both mechanisms are observed. The total acoustic disturbance in this case, is the sum of the two effects. Fig. 3b also demonstrates that the induced strains arising

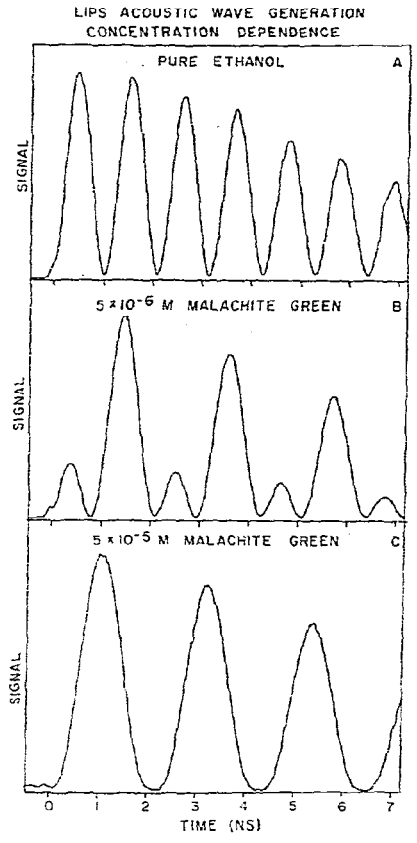

Fig. 3. LIPS transient grating data from pure ethanol and solutions of malachite green in ethanol. Excitation $\lambda = 532$ nm; probe $\lambda = 566$ nm. Fringe spacing $d = 2.47$ μm; acoustic cycle $\tau_{ac} = 2.13$ ns. Experimental conditions other than sample were identical throughout. (a) Pure ethanol. Electrostrictively-generated standing wave causes diffraction intensity to oscillate twice each acoustic cycle. (b) 5×10^{-6} M malachite green in ethanol. Electrostriction and optical absorption produce comparable responses. (c) 5×10^{-5} M malachite green in ethanol. Optical absorption effect dominates. Diffracted signal oscillates once each acoustic cycle.

from the two mechanisms are of opposite sign. If they were of the same sign, the first peak would be larger than the second, in contrast to the data [see eq. (18)].

To verify the quantitative aspects of the theoretical models for both mechanisms of LIPS generation, the value of the optoelastic constant, $\rho\, \partial n/\partial \rho$, of ethanol was determined using MG as the standard, following the procedure outlined in section 2.2.2. From eq. (20), the known values of the necessary constants ($q\gamma = 1$), k_2, and experimental determination of A/B in five separate measurements, we found $\rho\, \partial n/\partial \rho = 0.4 \pm 0.1$. This value is in good agreement with values in the literature (see table 1). The rather large uncertainty in the measurement originates from problems with the MG standard. It was found that at the very low concentrations necessary for the determination, the MG solution would become completely transparent in a couple of hours after preparation. This was observed first in the LIPS signal and later verified by measurement of the optical density using a Cary 17 spectrometer and a 10 cm cell. The discoloration is quite anomalous as [MG] = 10^{-4} M solutions can stand at room temperature for weeks with no change in optical density. This made determination of A/B difficult as all measurements had to be completed within 10 min in freshly prepared solutions. Nevertheless, the value of $\rho\, \partial n/\partial \rho$ is in agreement with the accepted value and its determination serves to confirm the LIPS theory as described in section 2. Thus, the theoretical description provides a quantitative account of the LIPS effect.

A better method for determining optoelastic constants using the LIPS technique, which avoids the use of absorption standards, uses a reference liquid with known optoelastic constant, as described in section 2.2.2. Table 1 gives the optoelastic constants of several liquids obtained in this manner, using eq. (21) and ethanol as the reference. In this experiment the signal obtained at $t = \frac{1}{4}\tau$ for the sample liquid is compared to that obtained for ethanol. The exact position of $\frac{1}{4}\tau$ depends on the speed of sound and was determined for each liquid by a time-resolved LIPS experiment which produced data like that in fig. 3a. Corrections to peak heights were made for some strongly damping liquids but this correction never resulted in more than a 3% change in the value of $\rho\, \partial n/\partial \rho$. Comparison of the experimental results obtained in this manner to the literature values in table 1 shows agreement to within $\approx$5% which is comparable to the agreements among the literature values.

Table 1 aiso lists the acoustic attenuation constants measured in the various liquids utilizing the temporal information provided in a LIPS experiment. All the constants obtained agree very well with measurements by other workers. Only the attenuation constants of

Table 1
Optoelastic and acoustic attenuation constants for liquids measured at 25°C [a]

Sample	Optoelastic constant $\rho\,\partial n/\partial\rho$			Acoustic attenuation $10^{17}\alpha/\nu^2$ (neper $cm^{-1}\,s^2$)		
	observed	literature		observed	literature	
ethanol	–	0.351 [10]	0.356 [11]	73 ± 6	65 [10]	55 [26]
methanol	0.320 ± 0.005	0.338 [12]	0.329 [13]	45 ± 4	30.2 [7]	–
carbon tetrachloride	0.48 ± 0.02	0.511 [10]	0.432 [14]	900 ± 100	550 [10]	545 [25]
chloroform	0.47 ± 0.01	0.459 [10]	0.470 [13]	880 ± 90	399 [10]	413 [25]
carbon disulphide	0.735 ± 0.005	0.715 [10]	0.712 [13]	995 ± 10	971 [24]	–
acetone	0.351 ± 0.004	0.351 [10]	0.356 [12]	82 ± 8	71 [10]	30 [27]
benzene	–	–	–	810 ± 30	818 [10]	840 [27]

[a] $\Lambda = 6.70\ \mu m$.

$CHCl_3$ and CCl_4 are significantly different due to the poor signal to noise ratio produced by those liquids.

LIPS may become an important experimental method for the measurement of acoustic attenuation and other acoustic observables due to the versatility it permits. Conventional pulse-echo and cw techniques [28] are limited to large sample dimensions by the physical size of the piezo-electric transducer used to generate the ultrasonics and generally requires mechanical contact with the sample. The LIPS technique, having nearly no size limitations, has great potential in the study of extremely small specimens such as fiber optics, phospholipid membranes, or domains of amorphous crystals.

In addition to making acoustic measurements, LIPS can also be used to measure very weak absorption spectra in a manner discussed in section 2.2.1. Fig. 4 shows a spectrum of the fifth vibrational overtone of the benzene C–H stretching mode. The spectrum was taken point by point, and the data have an appearance like those in fig. 3b. The spectral information is derived from the relative heights of the signal measured at $\frac{1}{4}\tau$ and $\frac{3}{4}\tau$. Eq. (19) was used to determine the parameter A/B at each wavelength.

The line shape and the position of λ_{max}, shown in fig. 4, are virtually identical to that obtained by an earlier thermal lensing study [29]. The spectrum quality is only moderate, mainly because the dye laser system employed was not constructed to be readily tuned over a wide wavelength range. However, the important feature is that this spectrum was taken with an effective path length of only 1 mm, i.e. a maximum optical density of $\approx 1 \times 10^{-5}$ (optical densities at least as low as 10^{-7} are measurable), demonstrating the very sensitive nature of the method.

LIPS as a tool for absorption spectroscopy shares a common feature with optoacoustic spectroscopy [30] in that it detects the absorption of light by nonradiative relaxation processes which produce phonons. However, in a LIPS measurement the phonons are generated coherently, which provides the potential for the increased sensitivity that usually accompanies coherent measurements.

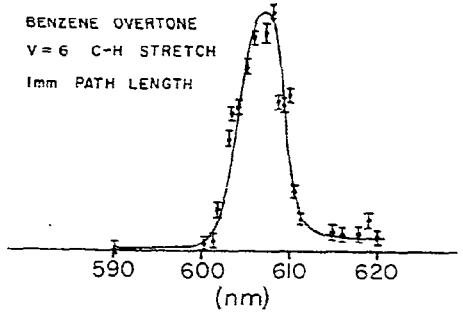

Fig. 4. A spectrum of the $\upsilon = 6$ transition of a C–H stretch of benzene in a 1 mm path of pure benzene. The spectrum is obtained from the LIPS transient grating experiment as a function of excitation wavelength for a fixed probe pulse wavelength. The data have an appearance like those of fig. 3b. The strength of the acoustic response at any wavelength is directly related to the absorptivity. Thus the technique is a type of coherent optoacoustic spectroscopy.

5. Concluding remarks

In this paper we have demonstrated the application of the laser-induced phonons method to the measurement of weak absorptions, optoelastic constants, and acoustic attenuation parameters. These measurements have also quantitatively confirmed the theoretical descriptions of the two LIPS excitation mechanisms, stimulated Brillouin scattering and absorptive heating. The experiments presented here concentrated on liquids, but the effect has also been observed in other media, e.g. solids and phospholipid bilayers. The method provides a technique for the optical generation of ultrasonic waves tunable over many orders of magnitude. Previously it has been demonstrated that the acoustic waves, once generated, can also be optically amplified, cancelled or phase shifted. Thus LIPS may find applications in optical communications and optical logic. Since it is not necessary to make mechanical contact to the sample, LIPS may be useful in material testing in situations in which conventional acoustic techniques are impractical. Finally, the technique should prove useful in the study of excited state–phonon interactions, lattice dynamical properties (including phase transitions), and processes which can be probed by acoustic waves.

Acknowledgement

RJDM would like to thank the Natural Sciences and Engineering Research Council of Canada for a postgraduate scholarship. RC would like to acknowledge a NATO Postdoctoral Fellowship. We would like to thank the National Science Foundation (DMR 79-20380) for support of this research.

References

[1] K.A. Nelson and M.D. Fayer, J. Chem. Phys. 72 (1980) 5202.
[2] K.A. Nelson, D.R. Lutz, L. Madison and M.D. Fayer, Phys. Rev. B24 (1981) 3261.
[3] K.A. Nelson, R.J.D. Miller, D.R. Lutz and M.D. Fayer, J. Appl. Phys. 53 (1982) 1144.
[4] K.A. Nelson, R. Casalegno, R.J.D. Miller and M.D. Fayer, J. Chem. Phys. 77 (1982) 1144.
[5] W. Kaiser and M. Maier, in: Laser handbook, Vol. 2, eds. F.T. Arecchi and E.O. Schulz-Dubois (North-Holland, Amsterdam, 1972) p. 1116.
[6] B.A. Auld, Acoustic fields and waves in solids, Vol. 1 (Wiley, New York, 1973).
[7] American Institute of Physics Handbook, 3rd Ed., ed. D.E. Gray (McGraw-Hill, New York, 1972).
[8] D.E. Caddes, C.F. Quate and C.D.W. Wilkinson, Appl. Phys. Letters 8 (1966) 309.
[9] J.F. Nye, Physical properties of crystals (Oxford Univ. Press, London, 1976).
[10] N. Uchida, Japan J. Appl. Phys. 7 (1968) 1259. 1259.
[11] F.E. Poindexter and J.S. Rosen, Phys. Rev. 45 (1934) 760.
[12] C.V. Raman and N.S. Nath, Proc. Indian Acad. Sci. A2 (1935) 406.
[13] R.M. Waxler and C.E. Weir, J. Res. Natl. Bur. Std. US 67A (1963) 163.
[14] W.A. Riley and W.R. Klein, J. Acoust. Soc. Am. 42 (1967) 1258.
[15] H. Mueller, Physics 6 (1935) 179.
[16] R.J.D. Miller, Ph. D. Thesis, Stanford University.
[17] K. Vedam and P. Limsuwan, J. Chem. Phys. 69 (1978) 4762.
[18] R. Lipelles and D. Kivelson, J. Chem. Phys. 67 (1977) 4564.
[19] H. Kogelnik, Bell System Tech. J. 48 (1969) 2909.
[20] A.B. Bathia and W.J. Noble, Proc. Roy. Soc. A220 (1953) 356.
[21] W.R. Klein and B.D. Cook, IEEE Trans. SU-14 (1967) 123.
[22] A.J. Matheson, Molecular acoustics (Wiley, New York, 1971).
[23] E.P. Ippen, C.V. Shank and A. Bergman, Chem. Phys. Letters 38 (1976) 611.
[24] K.F. Hertzfeld and T.A. Litovitz, Absorption and dispersion of ultrasonic waves (Academic Press, New York, 1959).
[25] A.A. Berdyev and B. Khemraev, Russian J. Phys. Chem. 41 (1967) 1490.
[26] W. Schaaffs, Landolt–Börnstein, Group 2, Vol. 5, Molecular acoustics (Springer, Berlin, 1967).
[27] D.F. Evans, J. Thomas, J.A. Nadas and M.A. Matesich, J. Phys. Chem. 75 (1971) 1714.
[28] E.P. Papadakis, Physical acoustics, Vol. 12, eds. W.P. Mason and R.N. Thurston (Academic Press, New York, 1976).
[29] M.E. Long, R.L. Swofford and A.C. Albrecht, Science 191 (1973) 183.
[30] C.K.N. Patel, A.C. Tam and R.J. Kerl, J. Chem. Phys. 71 (1979) 1470.